LIP-STUDENTS-25-08

Science Planning and Operations of the ESA JUICE Mission Radiation Monitor

Filipe Rodrigues[1,a]

[1] *Instituto Superior Técnico*

Project supervisor: Marco Pinto

Abstract. This work presents a planning study for characterizing the radiation environment during the JUICE mission. The analysis considers the effect of solar activity and heliocentric distance to the galactic cosmic ray ion population. Special attention is given to identifying optimal time intervals for the observation of specific particle species.
Keywords: JUICE, cosmic rays, solar modulation, radiation environment

1 Introduction

The JUpiter ICy moons Explorer (JUICE), part of the ESA Cosmic Vision program, is the first large-class mission dedicated to the Jovian system. Its primary objective is to investigate Jupiter and its icy moons, with a focus on the formation and evolution of giant planets and their potential habitability. JUICE also provides an opportunity to investigate the interplanetary radiation environment, a critical aspect for both spacecraft design and future exploration missions.

1.1 The RADEM Instrument

The RADiation–hard Electron Monitor (RADEM) is one of the instruments on board JUICE. The mission was launched the 14th of April 2023 and provides continuous measurements of the energetic particle environment. RADEM consists of three detector subsystems: the Electron Detector Head, the Proton and Heavy Ion Detector Head, and the Directional Detector Head. Together, these enable in situ measurements of electron, proton, and heavy ion fluxes over wide energy ranges.

1.1.1 Working principle

RADEM measures electrons in the 0.3–40 MeV range, protons in the 5–250 MeV range, and heavy ions between $\approx$ 7 MeV to $\approx$ 600 MeV. The sensors are connected to the low-gain channels of the RADEM front-end electronics, enabling the measurement of heavy ions from hydrogen up to oxygen. It can also measure ions with larger atomic number. However, due to its single threshold per diode, the instrument detects all ions above a given mass simultaneously. While different coincidence and anti-coincidence configurations between the sensors could allow to identify specific ion populations, the first sensor is unresponsive since launch. Such configurations require careful telecommanding and will be optimized during the mission.

The threshold of the deposited energies is progammable, changing the Response Function (RF) of the detector.

[a]e-mail: filipembr2001@gmail.com

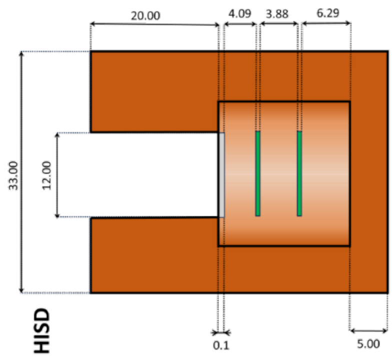

Figure 1. Schematic representation of the ion detector configuration in RADEM.5

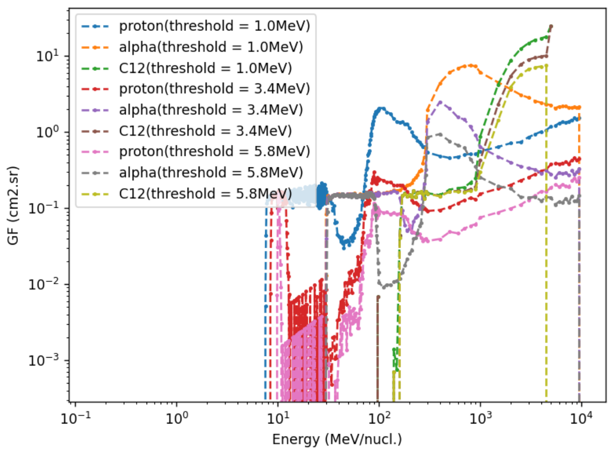

Figure 2. Some examples of different RFs.

2 Cosmic Rays

The characterization of galactic rays (GCRs) during the JUICE mission requires consideration of solar activity and heliocentric distance, as both strongly modulate the observed fluxes.

2.0.1 Solar Cycles

Solar activity follows an approximately 11-year cycle. During solar maximum, enhanced magnetic activity and solar wind conditions lead to a stronger modulation of galactic cosmic rays, reducing their flux in the inner heliosphere. Conversely, during solar minimum the reduced solar wind pressure allows for higher GCR intensities to reach 1 Astronomical Units (A.U.). JUICE was launched near solar maximum and will reach Jupiter close to a Solar minimum. That implies that is in a unique position to study the propagation of GCR from 1 to 5.2 A. U. over more than half of a solar cycle.

2.0.2 Distance from the Sun

The GCR flux also increases with the distance to the Sun. This has been measured by a few missions such as Voyager, Rosetta and Cassini. They determined that on average the rate is about 3%/A.U. but depends on the solar cycle. This effect can be approximated as:

$$\phi(d) = 1 + 0.03 \cdot (d - 1), \quad (1)$$

where d is the distance to the Sun in AU. For $d < 1$ AU the modulation is assumed to remain unchanged.

The spacecraft trajectory and corresponding heliocentric distance were obtained from NASA's ephemerides [1], shown in Fig. 3.

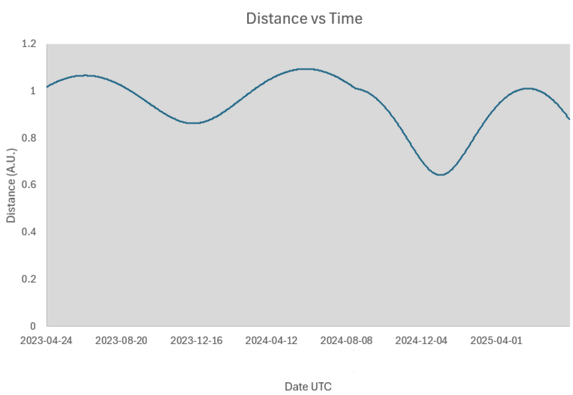

Figure 3. Heliocentric distance of JUICE along its mission timeline.

3 Solar Modulation Model

To estimate future modulation conditions during the JUICE mission, we extrapolated the modulation potential (ϕ) using the correlation between sunspot numbers and measured ϕ values.

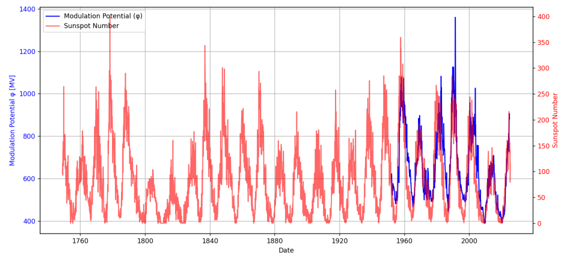

Figure 4. Time evolution of sunspot numbers and modulation potential.

The modulation potential since 19XX is shown in blue. The Sunspot number is shown in red. It dates back to XXXX.

The two quantities show a clear correlation, as illustrated in Fig. 5. The relationship was parameterized using a logarithmic model:

$$\phi = a \log(N + 1) + b, \quad (2)$$

where N is the number of sunspots. This model was then used to extrapolate modulation conditions up to 2035, as shown in Fig. 6. As we can see, our model seems to reproduce the expected behavior of the modulation potential, with the exception of the boundaries where there are significant deviations. These deviations likely arise because, in reality, the correlation between sunspot numbers and the solar modulation potential does not follow a purely logarithmic dependence, as illustrated in Fig. 5.

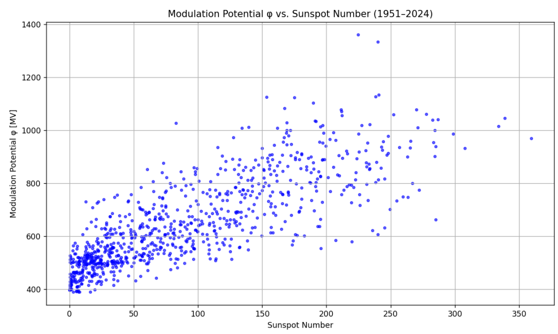

Figure 5. Correlation between sunspot numbers and solar modulation potential.

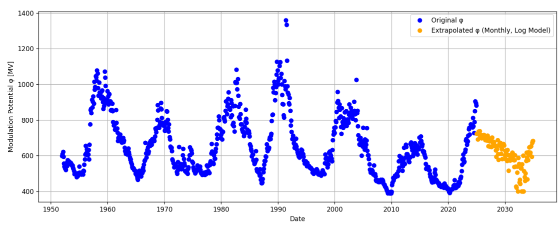

Figure 6. Extrapolated modulation potential until 2035.

4 Optimal Observation Periods for Different Particles

Based on the extrapolated modulation profile and the resulting particle flux distributions, it is possible to identify the energy ranges and mission intervals that are most suitable for the study of specific particle species. For each case, the statistical uncertainty is expected to follow the usual $\frac{1}{\sqrt{n}}$ behavior, where n is the number of detected counts.

To calculate the expected count rate, the following integral expression was used:

$$C_i = \int_0^\infty \phi(E), RF_i(E), dE, \tag{3}$$

where C_i represents the number of counts per second, $\phi(E)$ is the differential particle flux, and $RF_i(E)$ denotes the response function of the detector for the i-th configuration.

The observation time required to accumulate a total of N counts is then given by

$$T(d) = \frac{N/C_i}{24 \times 3600}, \tag{4}$$

where $T(d)$ is expressed in days. The denominator converts the expected accumulation time from seconds into days, assuming 24×3600 seconds per day.

It is important to note that, since one of the sensors has been unresponsive since launch, the instrument can only impose a minimum threshold value.

4.1 Threshold 0 MeV

In the lowest threshold energy interval (0 MeV), the particle flux is dominated by protons and alpha particles (Fig. 7). These species therefore represent the most favorable targets for detailed measurements in this range.

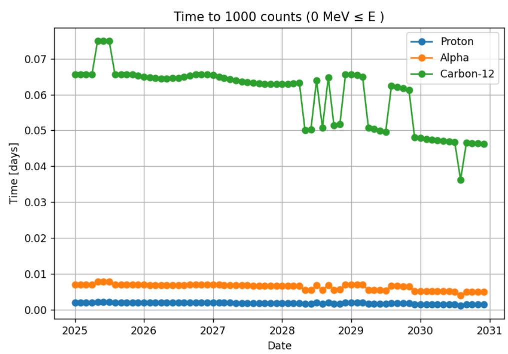

Figure 7. Simulated counts in the 0 MeV range (1000 counts).

4.2 Threshold 10 MeV

At intermediate energies (10 MeV), the spectra are strongly dominated by protons (Fig. 8). This range therefore provides the most suitable conditions for high-statistics proton studies.

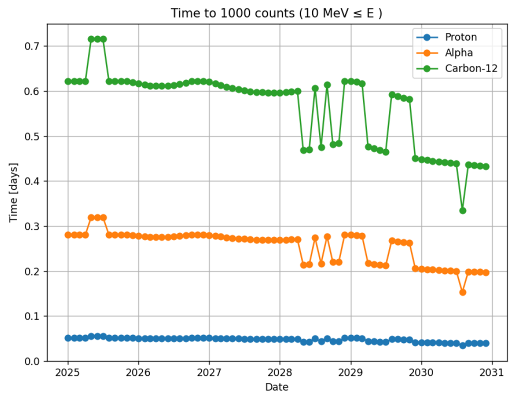

Figure 8. Simulated counts in the 10 MeV range (1000 counts).

4.3 Threshold 100 MeV

In the highest energy interval considered (100 MeV), the dominant contributions changes from protons to carbon-12 nuclei (Fig. 9). Although the statistics are lower compared to the previous ranges, this region enables the study of heavier nuclei.

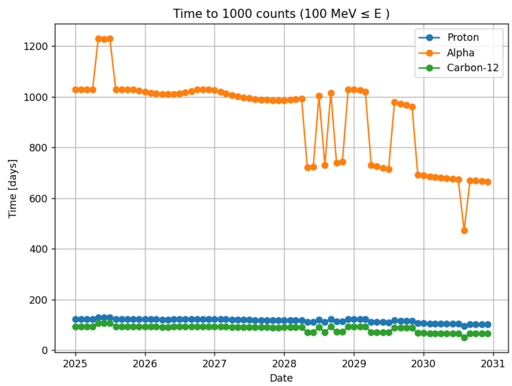

Figure 9. Simulated counts in the 100 MeV range (1000 counts).

4.4 Protons

From the analysis of all thresholds, it follows that the optimal conditions for proton studies are found from the 10 MeV onward. Here the proton flux is particularly intense, allowing statistical uncertainties at the level of 1% to be reached in short integration times (Fig. 10).

4.5 Alpha Particles

Alpha particle studies are most favorable in the 0 MeV range (Fig. 11). Due to the high flux levels, statistical uncertainties of about 1% can be achieved with relative ease.

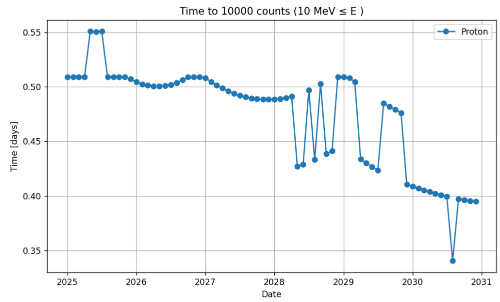

Figure 10. Proton counts for the 10 MeV (10,000 counts).

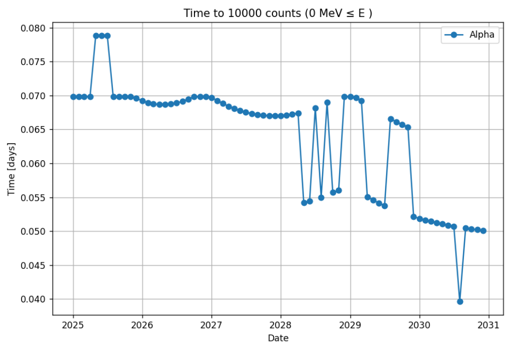

Figure 11. Alpha particle counts in the 0 MeV range (10,000 counts).

4.6 Carbon-12 Nuclei

Carbon-12 nuclei are best observed in the 100 MeV onward interval (Fig. 12). However, the relatively low flux limits the achievable statistics. For a reasonable observation time, the maximum number of counts is approximately 330, corresponding to a statistical uncertainty of about 5.5%.

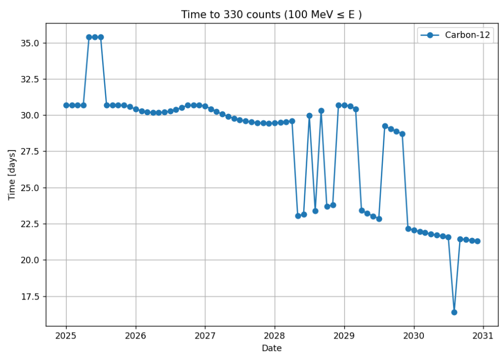

Figure 12. Carbon-12 counts in the 100 MeV range (330 counts).

5 Conclusions

We presented a framework for planning the study of the radiation environment during the JUICE mission. By accounting for solar cycle variability and heliocentric distance, we established a model that estimates modulation conditions throughout the mission timeline. The analysis provides guidance for identifying optimal periods for observing specific GCR particle species.

Our results indicate that proton and alpha particle populations can be studied with high statistical significance across most thresholds, especially at lower energies where flux levels are elevated and statistical uncertainties can reach the 1% level within relatively short observation times. In contrast, the characterization of heavier nuclei such as carbon-12 is considerably more challenging due to their reduced flux at high thresholds. Even under favorable conditions, the attainable statistics remain limited, leading to uncertainties above 5%, which hinders a precise determination of their spatial gradients. This highlights a fundamental trade-off between achievable statistics and particle mass when planning long-term GCR studies.

From an operational perspective, the results provide practical guidance for the configuration of RADEM during different mission phases. In particular, they identify optimal intervals and thresholds for maximizing the scientific return while accounting for solar cycle evolution and the gradual increase in heliocentric distance. Although the unresponsiveness of one of the sensors restricts the ability to finely tune coincidence configurations, the present analysis shows that meaningful and statistically robust measurements of protons and alpha particles remain feasible throughout the JUICE mission.

Future work will focus on refining the extrapolation of the modulation potential using real-time RADEM measurements and complementary solar activity indices. Furthermore, extending the analysis to heavier ions beyond carbon will be essential for constraining the contribution of GCR nuclei to the radiation environment at Jupiter. Such efforts will enhance the long-term predictive capability of the model and contribute to the preparation of future deep-space missions where radiation hazards are a critical design driver.

References

[1] NASA State Vector, http://spice.esac.esa.int/webgeocalc/#StateVector

[SILSO] SILSO, International Sunspot Number Monthly Bulletin, https://www.sidc.be/SILSO/datafiles

[Springer] Springer Nature, https://link.springer.com/article/10.1007/s11214-025-01163-9